Nano World Journal

https://doi.org/10.17756/nwj.2023-s3-031

Research Article

Open Access

Investigation on Tensile Strength of Novel Non-heat-treatable Aluminium AA5083 Alloy Reinforced with and without SiC During Friction Stir Welding Process

Napa Saikiran and Ravi Manikandan*

Department of Mechanical Engineering, Saveetha School of Engineering, Saveetha Institute of Medical and Technical Sciences, Saveetha University, Chennai, Tamil Nadu, India

***Correspondence to:**

Ravi Manikandan
Department of Mechanical Engineering,
Saveetha School of Engineering,
Saveetha Institute of Medical and Technical Sciences,
Saveetha University,
Chennai, Tamil Nadu, India.
E-mail: manikandanr.sse@saveetha.com

Received: July 27, 2023
Accepted: September 29, 2023
Published: October 05, 2023

Citation: Saikiran N, Manikandan R. 2023. Investigation on Tensile Strength of Novel Non-heat-treatable Aluminium AA5083 Alloy Reinforced with and without SiC During Friction Stir Welding Process. *NanoWorld J* 9(S3): S157-S161.

Published by United Scientific Group

Abstract

The primary objective of this study is to investigate the influence of SiC (Silicon carbide) nanoparticle reinforcement on the non-heat-treatable AA5083-H111 alloys to enhance the tensile strength of the friction stir welded joint. Using a universal testing machine, tensile tests were performed on the FSW (Friction Stir Welding) of AA5083-H111 aluminum in combination with SiC-reinforced butt joints. The statistical investigation followed the control group (AA5083-H111) and the experimental group (AA5083-H111 with SiC reinforcement). A PCBN (Polycrystalline Cubic Boron Nitride) tool, measuring 18 mm in diameter with a pin diameter of 6 mm and a height of 5.6 mm, was utilized for the experimental investigation of FSW. The sample size comprised 40 samples divided into two groups of 20. Independent sample testing was conducted with a statistical power of 80%. The AA5083-H111/SiC friction welded joint exhibits a maximum tensile strength of 365.22 MPa, surpassing the matrix materials by 30.3%. The statistical result found that AA5083-H111/SiC alloy achieved higher tensile strength than AA5083-H111 alloy with a significant value of two-tailed test $p = 0.048$ ($p < 0.05$) with a 95% confidence interval (CI). Statistically significant differences exist between the groups, as mentioned above. FSW of AA5083-H111 with SiC nanoparticles has displayed noteworthy assimilation of nanoparticles within the weld nugget zone. Nevertheless, it was observed that a high rotating speed of 1200 rpm coupled with an intermediate transverse speed of 60 mm/min has resulted in an enhanced tensile strength of the FSW joint.

Keywords

Friction stir welding, AA5083-H111, Tensile strength, Silicon carbide, Sustainable production

Introduction

FSW represents a highly efficient solid-state welding procedure employed to join any potential combination of dissimilar aluminum alloys [1]. There has been a growing need to minimize equipment size in the automotive and aviation sectors to improve fuel economy. As a result, lightly metallic and composite materials such as aluminum and superalloys are required [2]. The need for these studies on Al metal matrix composites (MMCs) has recently expanded due to their exceptional toughness, high performance, and high durability. Various researchers have found that FSW can significantly reduce the diameter of the HAZ and the extent of heat treatment in the welded joint of sustainable production [3].

By including hardened ceramics into the original raw material, a subset of the FSW and friction stir processing may be efficiently used to make MMCs [4]. Furthermore, studied the AA6082 reinforced by TiB_2 [5] and AA6061

composites reinforced with Al_2O_3 and carbon nanotubes [6] and AA5052-TiO_2 examined the formation of TiO_2, MgO, and Al_3Ti [7], whereas magnesium with ZrO_2 composites also fabricated [8, 9]. Numerous attempts have been made to combine FSW and processing by incorporating stiff ceramics into the weld nugget of the surfaces to be joined. Bahrami et al. [8] investigated AA7075 reinforced with SiC hard ceramic particles. The results were encouraging, as the material's ultimate tensile strength and elongation increased by 31 and 76.1%, respectively, compared to the same unwrought welded specimen [10]. Using an equally hard ceramic in the AA5083 metallic matrix allowed the researchers to improve the fracture toughness of the welding direction. SiC nanostructures and carbon nanotubes were mixed as matrix materials [11]. The final properties of the produced nanocomposite depend on the controlling parameters. However, it is an effective approach for dispersing various phases throughout the surface area of a plate [12].

Many researchers have not investigated the fabrication of reinforcement particle-filled grooves to produce micro- and nano-scale materials through FSW [13]. FSW can join MMCs, dependent upon the accessibility of materials in sustainable production. The primary similarity between these procedures is that they all enhance the nanocomposite in different ways, accounting for material flow, different compositions, and extreme deformations forced by the rotating tool during FSW. This study aimed to determine the effect of FSW on the tensile strength of aluminum MMCs reinforced with varied quantities of SiC particles of different sizes.

Materials and Method

The study was conducted within the CNC industries in the Saveetha School of Engineering, a subsidiary of Chennai's distinguished. The rolled sheets of aluminum alloy (AA5083-H111) of 6 mm thickness were divided into the desired size (150 mm x 150 mm x 6 mm) by the conventional machining process. The AA5083-H111 was used as the base material, and SiC was preferred as the reinforcement material. A total sample size of 40 specimens was used in this investigation, and each group carries 20 samples.

Group 1, the aluminum alloy was machined to dimensions of 150 mm x 150 mm x 6 mm, respectively. A square butt joint system is designed to produce FSW joints for various process parameters. The initial joint design was prepared by mechanically clamping the surface at both ends of the AA5083-H111 plates.

Group 2, two 6 mm thick and wide sheets of AA5083-H111 with SiC reinforcement for the plate dimension 150 mm long and 75 mm wide, with groove dimension 1 x 2 mm, were placed between adjacent faces. After insertion, the SiC nanoparticles were firmly pushed into the groove. The device was cast into a SiC-filled cavity.

According to the tensile sample processing, the top faces of the junctions were polished to minimize the marks developed by the shoulder. Tensile tests were carried out at a 1 mm/min crosshead velocity. Under changing process settings, the FSW joint was formed using a square butt joint design. The first joint arrangement was achieved by fastening the surface with mechanical clamps. The joints were manufactured using a pass welding operation. Weld joints are made using non-consumable PCBN tools. The joints were made with a domestically produced and manufactured machine (20 HP; 4000 RPM; 30 kN). SiC particles, possessing an average diameter of 45 µm, were employed as the reinforcements in the present study. To facilitate the attachment of the adhesive to the spray, pre-application of nanoparticles onto the substrates was carried out.

Statistical analysis

Statistical analysis software (Statistical Package for the Social Sciences) was performed to evaluate the tensile strength of aluminum (AA5083-H111) alloys. The significance ($p < 0.05$) and 95% CI between the two groups were identified by an independent t-test. The tensile strength value of the (AA5083-H111/SiC) developed mathematical model was compared to group 1 without SiC reinforcement. The response of tensile strength as a dependent variable is shown in the vertical axis [3].

Results

An experiment was conducted to investigate the impact of different concentrations of SiC on the tensile strength and percent elongation of AA5083-H111 base materials and welded AA5083-H111/SiC specimens. Table 1 and table 2 show the mechanical and chemical properties of AA5083-H111 aluminum alloy, whereas table 3 shows the mechanical and thermal properties of SiC reinforcement. The results of the tensile strength of the joint that has undergone FSW have been tabulated in table 4. Additionally, a comparative analysis between the control and experimental groups has been presented in table 5, wherein statistical data has been utilized to determine their respective tensile strengths. Additionally, table 6 displays the outcomes of the independent t-test, which exhibits statistical significance. Specimens with reinforcement particles have a higher tensile strength than those without SiC nanoparticles.

Table 1: Chemical composition of aluminum alloys (AA5083-H111).

Element	Mg	Mn	Zn	Fe	Cu	Si	Cr	Al
AA5083-H111	0.01	0.27	5.1	0.13	6.7	0.01	1.2	Bal

Table 2: Mechanical properties of aluminum alloys (AA5083-H111).

Element	Yield strength (MPa)	Tensile strength (MPa)	Elongation (%)
AA5083-H111	387	471	20

The operational mechanisms of the FSW methodology are demonstrated in figure 1. Subsequently, figure 2 illustrates that the ASTM E8M-04 was utilized to establish typical tensile samples. Figure 3 presents PCBN tool design along with graphical dimensions. Tensile strength of the FSW AA5083 aluminum alloy with respect to welding velocity is demonstrated in figure 4. Figure 5 shows vertical milling machine

Table 3: Mechanical and thermal properties of SiC.

Properties	Value
Melting point	2730 °C
Thermal conductivity	120 W/m-K
Poisson's ratio	0.35
Density	3.22 g/cm^3
Modulus of elasticity	90 GPa
Yield strength	21 GPa
Tensile strength	0.1379 GPa

Table 4: Tensile strength (MPa) results of group 1 (AA5083H111) and group 2 (AA5083- H111/SiC) of friction welded joint for different welding parameters.

S. No.	AA5083-H111	AA5083-H111/SiC
1	135.26	165.72
2	157.21	180.26
3	165.24	196.47
4	172.41	212.53
5	184.23	222.56
6	192.34	235.32
7	210.26	245.62
8	168.92	264.32
9	254.32	260.54
10	148.46	235.85
11	168.94	192.53
12	260.24	254.21
13	272.15	265.38
14	265.24	278.94
15	270.51	286.52
16	281.42	294.63
17	282.46	322.52
18	284.63	346.59
19	285.34	355.45
20	288.24	365.32

Table 5: Group statistics obtained of tensile strength obtained between AA5083-H111 (Group 1) and AA5083-H111/SiC (Group 2) of welded joint.

	Methods	N	Mean	Std. deviation	Std. error mean
Tensile strength (MPa)	1	20	222.91	56.455	12.62
	2	20	259.06	57.50	12.85

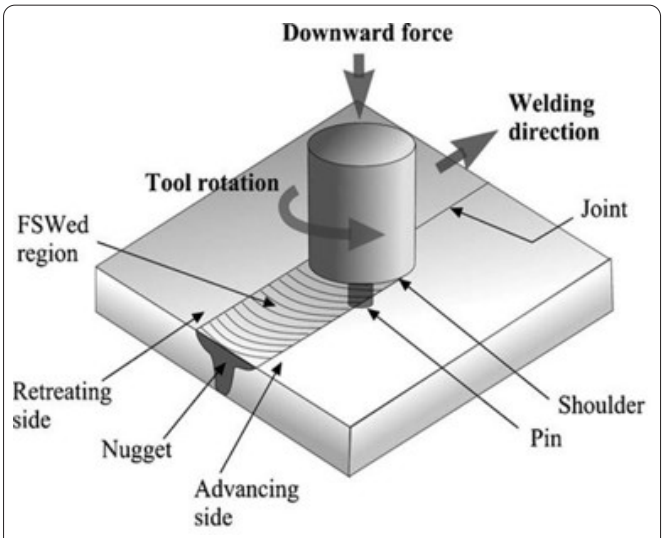

Figure 1: Schematic representation of FSW setup with various heat-affected welded zones.

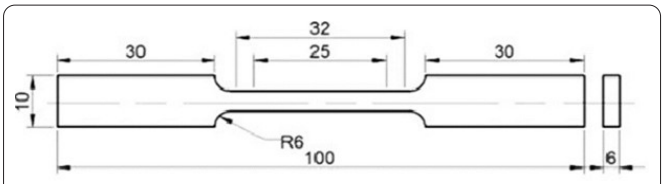

Figure 2: Dimension of tensile test specimen as per the ASTM E8M standard.

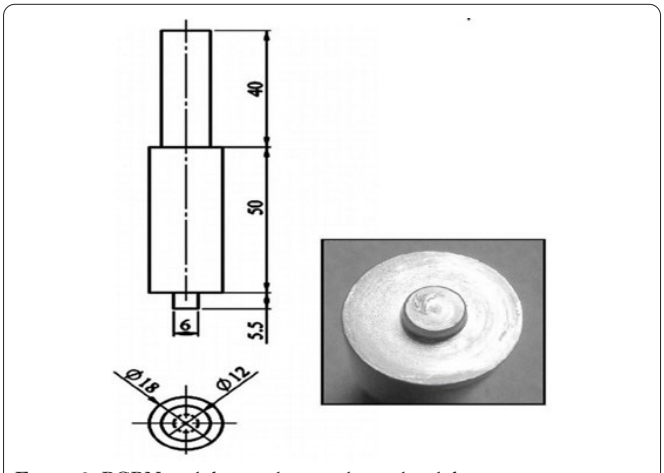

Figure 3: PCBN tool design along with graphical dimension.

for machining for FSW. The setup utilized for FSW is presented in figure 6. The prior and subsequent tensile specimens of the FSW joint are depicted in figure 7. The illustration of the correlation observed between the experimental groups is presented in figure 8.

Table 6: Levene's test for equality of variance and t-test for equality of means for tensile strength of group 1 and group 2.

		Levene's test for equality of variances		T-test for equality of means						
		F	Sig.	t	df	Sig. (2-tailed)	Mean difference	Std. error difference	95% CI of the difference	
									Lower	Upper
Tensile strength (MPa)	Equal variance assumed	0.690	0.411	-2.043	38	0.048	-36.67	17.95	-73.01	-0.330
	Equal variance not assumed			-2.043	37.97	0.048	-36.67	17.95	-73.01	-0.331

Figure 4: Friction welded joint for rotational speed 1200 rpm, translation speed 60 mm/min, and axial load 10 kN.

Figure 5: Vertical milling machine for machining for FSW.

Figure 6: Schematic representation of universal testing machine.

The ultimate tensile strength of AA5083-H111/SiC (Group 2) was 365.32 MPa, 18.46% lower than that of AA5083-H111 (265 MPa) aluminum alloys (Group 1), as shown in table 4. The highest tensile strength was achieved for SiC-reinforced aluminum alloys of 365.32 MPa, higher than 265 MPa, and a 22.64% increase in joint efficiency. The increasing concentrations of SiC (0.2%, 0.4%, and 0.6%) reinforcement increases the tensile strength (170 MPa - 365 MPa) of the AA5083-H111 friction welded joint, respectively. During the tensile test, the percentage of elongation value of each specimen was recorded by a computerized digital recorder system. The elongation percentage for the aluminum composites AA5083-H111 is 15.66, which was lower than that of AA5083-H111 (23.54) without SiC reinforcement.

Discussion

According to Uematsu et al. [14], the sensibility of the base material, tool rotation, and transverse speed may increase strength properties. Although the tensile strength is lost during the FSW process, cold-worked or precipitation-hardened aluminum often exhibits the lowest elongation achieved in a welded joint. The high welding efficiency produced due to the selected welding speed is considered a performance and service quality to provide good weldability of aluminum alloys in industrial applications [15]. Tensile fracture results revealed that the NZ-TMZ on the retreating side had damaged similar elements. Tensile testing revealed a fracture on the retreating side, highlighting the sensitivity of this zone compared to the advancing side. Dislocations arise at the interface of the AA5083 matrix and SiC nanoparticles due to the disparate coefficients of thermal expansion between the two materials. As can be observed, the single-pass weld pattern is characteristic, and the FSW pattern fractures without using SiC nanoparticles [2].

When compared with group 1 (AA5083-H111), the tensile strength of group 2 (AA5083-H111) with SiC reinforcement friction welded joint significantly increased, as ensured by achieved p value 0.048 (Significance $p < 0.05$), as shown in table 5. The high rotational and medium translational speeds (1200 rpm, 60 mm/min, and axial load 8 kN) achieved the highest tensile strength for AA5083-H111 with SiC reinforced friction welded joint. Figure 7 shows the mean tensile strength at 95% CI with +/- 1 standard deviation for both experimental and control groups. Lower rotational speed and translation speed lead to lower tensile strength when compared to high rotational speed and medium translation speeds [8]

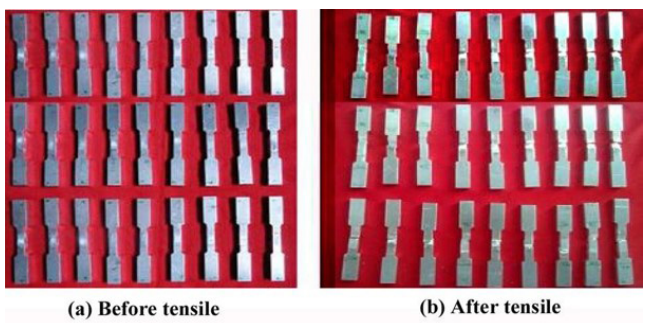

Figure 7: Representation of tensile specimen of **(a)** before and **(b)** after tensile specimen fractures.

Based on the machine speed used for joint manufacturing, all joints have a tensile strength greater than the parent material. When exposed to a tool rotation rate of 1200 rpm, the AA5083-H111 compound exhibits improved tensile characteristics compared to other rotational speeds. The impact of tool rotation speed on the stress parameters of FSW AA5083-H111 aluminum alloy is depicted in figure 6. A moderate rotating speed achieves optimal tensile strength in FSW joints (at 1200 rpm). Rotational and translational speeds both have an impact on the tensile characteristics of connections and fracture locations [16]. The imperfections within the FSW region, such as cavities, fissures, tunnels, or fractures, result in joint defects. These defects are accompanied by site failures that displace towards the lower hardness region zone in the absence of any defects [3]. Effect of tool rotational speed on tensile strength FSW junctions decrease their tensile strength, At high welding speeds (20 mm/min). The joint's tensile strength experiences a decrease upon surpassing a welding speed of 40 mm/min. This observable trend persists across all connections, irrespective of the tool pin's profile. The tensile potency of the FSW of AA5083 is enhanced, and the FSW of AA5083 exhibits exceptional structural grain configurations devoid of any imperfections. FSW has a moderate temperature increase and does not melt the metal surface.

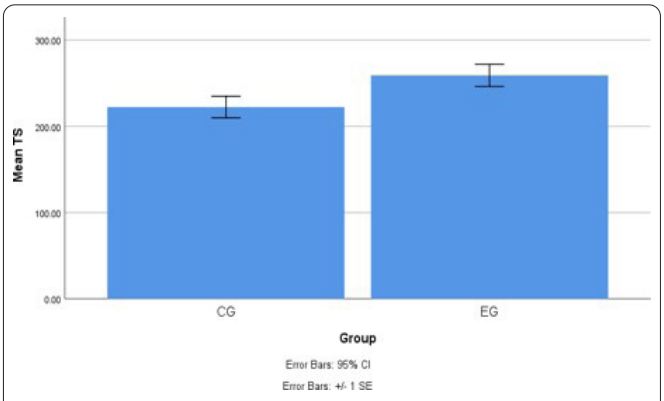

Figure 8: Correlation of the experimental and the control groups' rates of tensile strength. The specimens of the control group of machining performance using novel AA5083-H111/SiC had higher tensile strength (365.32 MPa) and a lower standard deviation than the samples of the experimental group with the AA5083-H111 without SiC reinforcement (285.34MPa). X-axis: AA5083-H111(Group 1) and AA5083-H111 (Group 2); Y-axis: mean MRR with +/-1 standard deviation of error.

Conclusion

The AA5083-H111 alloy, when reinforced with SiC, has been found to exhibit an impressive maximum tensile strength of 365.32 MPa. This outcome was made possible by applying specific process parameters: a 1200 rpm tool rotational speed, a 60 mm/min translational speed, and an 8 kN axial load. Upon statistical analysis, it was determined that the tensile strength of the AA5083-H111 alloy with SiC reinforcement was significantly higher than that of the AA5083-H111 matrix alloy. Specifically, a two-tailed value of 0.048 ($p < 0.05$) at 95% CI was observed to be significant. It clearly shows the significant difference between the groups.

Acknowledgements

None.

Conflict of Interest

None.

References

1. Murr LE. 2010. A review of FSW research on dissimilar metal and alloy systems. *J Mater Eng Perform* 19: 1071-1089. https://doi.org/10.1007/s11665-010-9598-0
2. Salih OS, Ou H, Sun W, McCartney DG. 2015. A review of friction stir welding of aluminium matrix composites. *Mater Des* 86: 61-71. https://doi.org/10.1016/j.matdes.2015.07.071
3. Zuo L, Zhao X, Li Z, Zuo D, Wang H. 2020. A review of friction stir joining of SiC_p/Al composites. *Chinese J Aeronaut* 33(3): 792-804. https://doi.org/10.1016/j.cja.2019.07.019
4. Shafiei-Zarghani A, Kashani-Bozorg SF, Zarei-Hanzaki A. 2009. Microstructures and mechanical properties of Al/Al_2O_3 surface nano-composite layer produced by friction stir processing. *Mater Sci Engi A* 500(1-2): 84-91. https://doi.org/10.1016/j.msea.2008.09.064
5. Palanivel R, Dinaharan I, Laubscher RF, Davim JP. 2016. Influence of boron nitride nanoparticles on microstructure and wear behavior of AA6082/TiB_2 hybrid aluminum composites synthesized by friction stir processing. *Mater Des* 106: 195-204. https://doi.org/10.1016/j.matdes.2016.05.127
6. Du Z, Tan MJ, Guo JF, Bi G, Wei J. 2016. Fabrication of a new Al-Al_2O_3-CNTs composite using friction stir processing (FSP). *Mater Sci Eng A* 667: 125-131. https://doi.org/10.1016/j.msea.2016.04.094
7. Zangabad PS, Khodabakhshi F, Simchi A, Kokabi AH. 2016. Fatigue fracture of friction-stir processed Al-Al_3Ti-MgO hybrid nanocomposites. *Int J Fatigue* 87: 266-278. https://doi.org/10.1016/j.ijfatigue.2016.02.007
8. Bahrami M, Givi MKB, Dehghani K, Parvin N. 2014. On the role of pin geometry in microstructure and mechanical properties of AA7075/SiC nano-composite fabricated by friction stir welding technique. *Mater Des* 53: 519-527. https://doi.org/10.1016/j.matdes.2013.07.049
9. Navazani M, Dehghani K. 2016. Fabrication of Mg-ZrO_2 surface layer composites by friction stir processing. *J Mater Process Technol* 229: 439-449. https://doi.org/10.1016/j.jmatprotec.2015.09.047
10. Ahn B, Choi D, Kim Y, Jung S. 2012. Fabrication of SiC_p/AA5083 composite via friction stir welding. *Trans Nonferrous Met Soc China* 22: s634-s638. https://doi.org/10.1016/S1003-6326(12)61777-4
11. Pantelis DI, Karakizis PN, Daniolos NM, Charitidis CA, Koumoulos EP, et al. 2016. Microstructural study and mechanical properties of dissimilar friction stir welded AA5083-H111 and AA6082-T6 reinforced with SiC nanoparticles. *Mater Manuf Process* 31(3): 264-274. https://doi.org/10.1080/10426914.2015.1019095
12. Kurt A, Uygur I, Cete E. 2011. Surface modification of aluminium by friction stir processing. *J Mater Process Technol* 211(3): 313-317. https://doi.org/10.1016/j.jmatprotec.2010.09.020
13. Mishra RS, Mahoney MW, Sato Y, Hovanski Y. Friction Stir Welding and Processing VIII. Springer Cham.
14. Uematsu Y, Tokaji K, Shibata H, Tozaki Y, Ohmune T. 2009. Fatigue behaviour of friction stir welds without neither welding flash nor flaw in several aluminium alloys. *Int J Fatigue* 31(10): 1443-1453. https://doi.org/10.1016/j.ijfatigue.2009.06.015
15. Midhun S, Ramesh C, Chellamuthu K, Yokeswaran R. 2022. Dissimilar resistance spot welding process on AISI 304 and AISI 202 by investigation metals. *Mater Today Proc* 69: 1213-1217. https://doi.org/10.1016/j.matpr.2022.08.262
16. Yokeswaran R, Vijayan V, Karthikeyan T, Loganathan M, Antony AG. 2020. Microstructure analysis of IS2062 plates cladded with SS2594 by TIG welding process. *J New Mater Electrochem Syst* 23(4): 269-273. https://doi.org/10.14447/jnmes.v23i4.a08